Prevention of acid-induced sludge formation using an environmentally–friendly bio-based nonionic surfactant

Hamidreza Asaadian [a,*], Pouyan Ahmadi [b], Mohammad Zare Khormizi [c], Saba Mohammadi [c], Bahram Soltani Soulgani [c], Shirin Baghersaei [d], Babak Mokhtari [d]

[a] Department of Geoscience and Petroleum, Norwegian University of Science and Technology, Trondheim, Norway
[b] Department of Hydrogeology, Helmholtz-Centre for Environmental Research, UFZ, Leipzig, Germany
[c] Ahvaz Faculty of Petroleum, Petroleum University of Technology, Iran
[d] Department of Chemistry, Faculty of Science, Shahid Chamran University of Ahvaz, Iran

ARTICLE INFO

ABSTRACT

Asphaltene molecules are one of the main sub-fractions of heavy crude oils. During matrix acidizing operation, these polar molecules are highly susceptible to interact with acid and form a third phase called asphaltic sludge. Deposition of the formed sludge on the rock surface and plugging their pore throats alters the rock wettability state and consequently its permeability. In the present study, the impact of acid and oil on the volume of the formed sludge as well as on the wettability of three rock types including sandstone, fractured and vuggy carbonate rocks were experimentally explored. A new environmentally friendly bio-surfactant which is extracted from Zizyphus spina-christ shrub (ZSCS) leaves was used as an inhibitor to control the potential damage causing by wettability alteration and the following pore plugging. Two common commercial additives were also evaluated against the bio surfactant performance that was used in this study. As a complementary step, molecular dynamic simulations were also conducted firstly to shed the light on the affinities between asphaltene and acid molecules and then check how the presence of ZSCS intervene the interaction between asphaltene molecules and rock surface. Our findings prove that using ZSCS provides optimal solution concerning production issues (i.e., Prevention of acid-induced sludge formation), both economically and environmentally; economically as it simply costs less than other commonly used chemicals, and environmentally as it extracted from nature.

1. Introduction

Matrix and fracture acidizing are effective methods to achieve higher production rates like the other available stimulation techniques in carbonate oil and gas reservoirs (Morales and Diaz, 2017). Acids dissolve induced skin and increase the permeability of the near wellbore region by dissolving the rock by which opens the plugged pores by fines and/or in carbonated reservoirs creates penetrable channels called wormhole (Asaadian et al., 2017a). Matrix acidizing is typically designed in three different stages: pre-flush, main treatment, and over-flush. The rock surface of formation is prepared for a more efficient acid/rock reaction during the pre-flush stage (Karimi et al., 2018). The formation fluid is pushed back by the nonreactive fluid from the damaged zone to the reservoir. This stage has a critical effect on the formation of sludge and emulsion during the main treatment stage of stimulation. The success of any stimulation operation depends on the accurate prediction of the

sub-surface condition during the acidizing treatment (Asaadian and Soulgani, 2016; Abdollahi and Shadizadeh, 2012). Before acidizing execution, final studies on the spreading of the wormhole, fluid viscosity alteration, possible further treatment damages must be carried out. To this end, the knowledge of formation damage mechanisms, acid treatment and chemicals are required for a successful acidizing plan (McLeod, 1984; Garrouch and Jennings, 2017).

Hydrochloric acid (HCl) is commonly used as the base treatment fluid in carbonate reservoirs and while forms a mixture with hydrofluoric acid (HF), it has the same application in formations with sandstone rock type (Wong et al., 1996, 1997; Xie et al., 2005; Shafiq and Mahmud, 2017). After acid injection into the formation, the interaction between crude oil and acid cause two major damages named asphaltic sludge and rigid-film emulsion. Moore et al., 1965 studied the reason and the probability of sludge formation by conducting several laboratory experiments and examined stabilizing agents as prevention solution

---

* Corresponding author.
E-mail address: hamidreza.asaadian@ntnu.no (H. Asaadian).

method (Moore et al., 1965). These two forms of acid stimulation damages cause rock wettability alteration, pore plugging and phase trapping (Garrouch et al., 2006; Houchin et al., 1990; Aghajanzadeh et al., 2019). Furthermore, formed asphaltic sludge in the near wellbore makes the clean-up slower resulting in the disruption in oil production (Jacobs and Thorne, 1986).

Asphaltene, one of the main elements in forming the induced sludge process, is defined as the heaviest component of crude oil with high polarity and active surface with solubility in aromatic solvents such as toluene, benzene and insoluble in alkanes (Asaadian et al., 2017b; Ahmadi et al., 2019a; Azari et al., 2018). Asphaltene molecules are made of polycyclic aromatic hydrocarbon rings with peripheral alkane chains (Ahmadi et al., 2019b; Langevin and Argillier, 2016). Limited percentage of heteroatoms like N, O and S exist in the polyaromatic asphaltene molecules with paraffinic rings, alkyl linkage and aliphatic side chains decorating them. The following main functional groups are defined for existing heteroatoms. S: thiophene, sulfidric, sulfoxide; N: pyrrolic, pyridine, quinoline; and O: hydroxyl, carbonyl and carboxyl. Also, the brownish-black color of asphaltene molecules reflects the extended conjugation of aromatic structure (Adams, 2014; Shahsavani et al., 2019).

According to the charge of acid-base pairs, they may exist in the asphaltene molecules, normally between oxygen and the functional groups containing nitrogen. Metal porphyrins or related chelating metal structures are also present. The majority of these metal compounds are coordination complexes containing vanadium, nickel, and iron. Porphyrins (and metal complexes in general) are proven to contribute to fouling and are highly enriched in asphaltene deposits, despite their modest concentration. They are particularly troublesome as they can cross-link and become entrapped within asphaltene supramolecular structures, making them difficult to remove (Olayiwola and Dejam, 2019; Ayirala et al., 2006).

Several additives are used along with acids to prevent further damage due to unwanted possible reactions with equipment, rock and reservoir fluids and decrease the risk of sludge deposition in the pipelines (Weidner, 2011; Rabie and Nasr-El-Din, 2015; Frenier and Hill, 2002). When asphaltic sludge is formed, it is insoluble in most treating chemicals expect toluene. Hence, sludge removal from the formation is not as easy as wellbore clean-up because of the difficulties caused by solvent injection into the formation (Campbell, 2002; Lu et al., 2021). Therefore, prevention of sludge formation is preferred to curing. Anti-sludge agents that are used to prevent sludge formation are mostly alkyl phenols, fatty acids and certain oil-soluble surface-active agents (Houchin et al., 1990). Similarly, ionic and non-ionic surfactants encourage to maintain the asphaltene molecules in the organic phase (Olayiwola and Dejam, 2019). On the other hand, the probability of sludge precipitation on the reservoir rock poses the rock wettability alteration toward oil-wetting condition that is considered as subsidiary damage (Kudrashou and Nasr-El-Din, 2019). In this case, surfactants are used to keep the wettability intact or become more water-wet and stabilize the asphaltene molecules in pre-flush stage and reduce oil/water IFT in the main stage of the treatment (Taylor et al., 2003; Maley et al., 2015).

Many research groups have attempted in various ways to prevent asphaltene molecules from being aggregated in order to stop forming the induced sludge (AlMubarak et al., 2015; Almubarak et al., 2021; Khurshid et al., 2022; Shirazi et al., 2019). An ester of sulfonic acid, including such monoethoxylated dodecyl benzene sulfonic acid, was presented by Loony and McDougall in 1984 as an anti-sludge agent for acid stimulated hydrocarbon containing formations (Looney and McDougall, 1984). The compositions Dyer invented in 1997 contain an alkyl aryl sulfonic acid or salt thereof, a nonethoxylated glycol, and an acetylenic alcohol in an alkyl alcohol solvent. (Dyer, 1997). During acid treatment and stimulation of hydrocarbon wells, these compositions have proven to be helpful at controlling sludge and emulsion growth. Campbell (2002) invented certain formulations that involve the demulsification

and liquification of hydrocarbon-based sludges (Campbell, 2002). The innovation aims to create a hydrocarbon-based sludge that is enough liquefied to be pumped and sufficiently demulsified to facilitate the separation of the sludge's waters, oils, and solids (Campbell, 2002). Knopp (2009) composition demonstrated the ability to either inhibit or prevent the formation of emulsions during acid stimulation of hydrocarbon wells. It consists of an alkyldiphenyl oxide sulfonic acid or derivative thereof, an acetylenic alcohol, and an alkyl diphenyl oxide sulfonic acid or derivative thereof, all in an alkyl alcohol solvent (Knopp, 2009). Fogler and Chang studied crude oil asphaltene stabilization in 1981. Several factors have been found to be influential in the amphiphile's ability to stabilize crude oil asphaltenes, including the polarity of the headgroup and the length of the alkyl tail (Chang and Fogler, 1994). Furthermore, a study by O'Nill et al. (2015) compared anionic and cationic anti-sludge agents. They found that anionic anti-sludge surfactants control acid-induced precipitation more effectively than other surfactants. Additionally, cationic anti-sludge surfactants prevent precipitation in a different manner than anionic surfactants (O'Neil et al., 2015). There are wide ranges of surfactants that are used in oil well acidizing for anti-sludge and demulsifier agents (Table 1) (Hashmi and Firoozabadi, 2013; Mirvakili et al., 2012).

Additionally, several studies have been conducted to address bio-surfactant application in the petroleum industry (Bognolo, 1999; PordelShahri et al., 2012; Ahmadi et al., 2015; Ahmadi and Shadizadeh, 2013; Deymeh et al., 2012). Initially, Pordel Shahri et al., 2012 introduced a new type of surfactant which was extracted from the leaves of Zizyphus spina-christi (PordelShahri et al., 2012). Abdollahi et al. studied henna as an anti-corrosion additive in the acidizing sandstone rock (Abdollahi and Shadizadeh, 2012). Despite existence of the long literature review, there is still a lack of understanding of the nature and mechanisms of acid-induced sludge formation and prevention. In this study, has been attempted to present a proper insight into sludge nature and propose a novel environment-friendly surfactant to prevent sludge damages during matrix acidizing particularly alteration of rock properties like wettability. In addition, molecular dynamic simulations were also carried out to provide a thorough understanding of the underlying mechanisms contributing to the sludge occurrence and its remediation.

2. Material

In order to avoid a long passage, elaborating the procedures for all the experiments carried out in this paper, is provided in Supplementary Material (SM) (See Figs. S1–S5). The used materials in this study are described in the following sections. Each experiment's measurements are performed three times, and the presented data is the average of the results from each campaign. The experimental error for each experiment is shown by error bars in related figure.

2.1. Crude oil

The crude oil used in these experiments was from Asmari formation, one of the south-West Iranian oil reservoirs which irrespective of its low specific gravity, has a considerable asphaltene content. SARA test analysis on dead oil showed that the values of saturation, aromatic, resin and asphaltene sub-fractions of oil were 53.5, 16.5, 12 and 18 wt%, respectively. Also, the concentration of Fe, Ni, V and Ca ions were 700, 93, 370 and 530 ppm, respectively. Extracted asphaltene is used to prepare synthetic oils with specific weight percent of asphaltene content by mixing with toluene. Asmari oil was chosen because the similar molecular structure was present in the published articles (Takanohashi et al., 2004; Sheremata et al., 2004). Two simulated molecular structures similar to described crude oil are illustrated in Fig. 1b and c.

2.2. Nonionic bio-surfactant

A bio-surfactant is extracted from the leaves of Zizyphus spina-christi

Table 1
Common surfactants used as anti-sludge (Mirvakili et al., 2012).

|	Common Name	IUPAC name	Chemical Formula	Purity	Supplier
1	Dodecyl benzene sulfonic acid	4-dodecylbenzenesulfonic acid	$C_{12}H_{25}C_6H_4SO_3H$	0.98	Behdash Co.
2	Benzene sulfonic acid	Benzenesulfonic acid hydrate	$C_6H_8O_4S$	>0.99	Merck Co.
3	Toluene sulfonic acid	4-methylbenzenesulfonic acid hydrate	$CH_3C_6H_4SO_3H.H_2O$	>0.99	Merck Co.
4	Phenol sulfonic acid	4-hydroxybenzenesulfonic acid	$C_6H_6O_4S$	>0.99	Merck Co.
5	Ammonium acetate	Acetic acid ammoniate	$C_2H_7NO_2$	>0.99	Merck Co.
6	Didecyl dimethyl ammonium chloride	Didecyl-dimethylammonium chloride	$C_{22}H_{48}ClN$	>0.99	Merck Co.
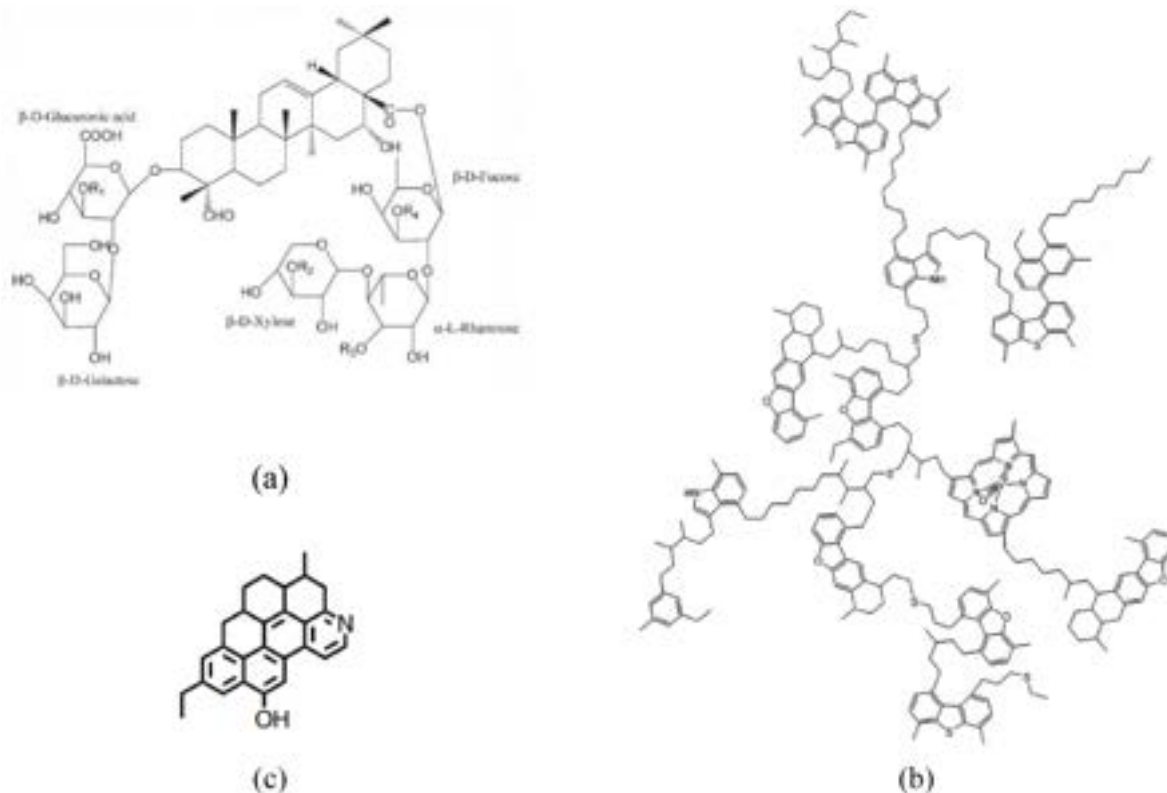
Fig. 1. 2D molecular structure of (a) Saponins, (b) Asphaltene type II and (c) Asphaltene type I (Ahmadi and Shadizadeh, 2013; Takanohashi et al., 2004; Sheremata et al., 2004).

shrub. It has a light-gray, cracked and scaly bark. Its leaf surface is also glabrous on top and finely pubescent below. It can be widely found in the Middle East especially in Iran, Iraq, Jordon, and Egypt. This plant-based material, which is a natural surface-active substance, was used as a surfactant in enhanced oil recovery research and also as shale swelling inhibitor in drilling studies previously conducted. However, utilizing this surfactant in matrix acidizing as anti-sludge has not yet been studied in the literature. Concentration of saponins, bio-surfactant, produced by more than 500 plant species, has been reported to be fairly high in leaves of Zizyphus spina-christi (PordelShahri et al., 2012; Stanimirova et al., 2011).

From the butanol extract of the leaves of the Z. spina-christi, four saponin glycosides were isolated: Christinin A, B, C, and D. Their structures were confirmed by chemical and FT-IR spectroscopic evidence. Christinin A was found to be 3-O-α-Lfucopyranosyl/β-D-glucopyranosyl/α-L-arabinopyranosyl jujubogenin. The others are new, Christinin B being 3-O-α-D-fucopyranosyl/β-D-glucopyranosyl-4-sulfate/alpha-L-arabinopyranosyl jujubogenin, Christinin C being 3-O-β-glucopyranosyl/α-L-rhamnopyranosyl/α-L-arabinopyranosyl jujubogenin, and Christinin D being 3-O-α-Lfucopyranosyl/β-D-arabinopyranosyl/β-D-glucopyranosyl/α-L-arabinopyranosyl jujubogenin. The saponins molecules have both hydrophobic and hydrophilic parts.

Triterpenoid and steroid or steroid-alkaloid are made hydrophobic part while the hydrophilic part is composed of saccharide residues. Both two parts are connected by glyco-side bonds (Stanimirova et al., 2011). Soxhlet apparatus is used to obtain soluble (in water and alcohol) dark brown powder with a density and pH value of 0.09 gr/cm3 and 5.8 respectively (Ayirala et al., 2006). A schematic of saponin chemical structure is illustrated in Fig. 1.

2.3. Thin sections

Three series of fourteen thin-sections are prepared from sandstone, fractured, and vuggy carbonate rocks (total 42 thin-sections). In order to simulate the actual condition of the reservoir for testing, these rocks are collected from outcrop reservoir formation and aged separately with brine and dead oil. The semi-quantitative mineral compositions of the three rock sets are determined by X-ray diffraction (XRD) are provided in Table 2.

2.4. Commercial additives

Two common commercial additives (i.e., WA120 and NE32) which are frequently used in field matrix acidizing operations are prepared and compared with bio-surfactants. WA 120 has been mostly used in pre-

Table 2
The semi-quantitative mineral compositions of the three rock sets by XRD.

Rock	XRD weight percent measurements (wt.%)				XRD-based grain density (g/cm3)
	Anhydrite	Calcite	Dolomite	Quartz	
Fractured Carbonate	0.00	98.58	0.64	0.78	2.710
Vuggy Carbonate	0.00	87.68	11.94	0.38	2.728
	Quartz	**K-Felspare**	**Plagioclase**	**Clay + Mica**	
Sandstone	73.23	11.82	10.03	4.92	2.671

flush stage to prevent wettability alteration during acidizing treatment, while NE32 is usually used during main treatment process as anti-sludge agent (McLeod, 1984; Garrouch and Jennings, 2017). All chemicals including n-heptane, toluene, and 37 wt% hydrochloric acid which are used in the following procedures, were provided from Merck Company.
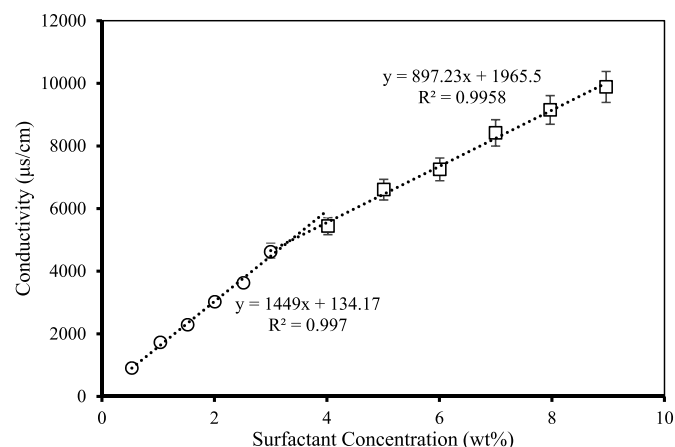
3. Results and discussion

3.1. Critical micelle concentration (CMC) measurement

In general, there are various methods for determining CMC; in this case, the conductivity approach was chosen. Because of the various degrees of surfactant ionization below and above the CMC, the conductivity trend of aqueous ionic surfactant solutions changes at the CMC. Surfactant monomers behave as strong electrolytes below the CMC and are slightly ionized above the micelles. The charge, mobility, and concentrations of all ions present in the solution are reflected in the specific conductance or conductivity (k) of the solution (Abdollahi and Shadizadeh, 2012). Concentrations of bio-surfactant ZSCE were varied from 0.5 to 9 wt% (1000–80,000 ppm). Conductivity of solutions was ranged from high concentration to low (Fig. 2). To determine the location of CMC, conductivity data are plotted against concentrations by which the turning point in the curve reveals the value of CMC. When concentration of surfactant solution increases to a certain value, its molecules will come to association reaction, and start to form micelles, hence a sharp change in trend of curve is observed (Fig. 2). Careful experimental measurements using highly purified systems revealed that somewhat gradual and continuous changes in physicochemical properties occurred near the CMC. The CMC value for bio-surfactant ZSCE was obtained round 3.32 wt%, which is used in experiments.

3.2. Adsorption experiment

Batch equilibrium testing on carbonate minerals is used to measure surfactant adsorption on reservoir rock. A given volume of bio-surfactant solution at a known concentration is combined with a specified quantity of crushed rock in a centrifuge tube in these studies on crushed core. After 1, 2, 3, 6, 12, and 24 h, samples of bio-surfactant solution were obtained from the container and residual concentration was determined using a conductivity meter. The system is in equilibrium and the test is completed when the concentration remains constant over time. Preliminary studies revealed that adsorption equilibrium could be established within 2 h (Fig. 3), which can be used to design aging experiments.

3.3. pH and refractive index measurement

In optics, the propagation of light through the medium is described by the refractive index. This dimensionless parameter is defined as:

$$n = c/\upsilon \qquad (1)$$

Where c is the light speed and υ is the light velocity in the medium. According to the definition of the refractive index, the existence of dispersed particles in medium increases the refractive index by lowering the speed of light through media (Singh, 2002). Therefore, this parameter is used to determine the concentration of asphaltene molecules in the solutions. Thus, by sampling a few amounts of prepared synthetic oils and determining their refractive index, an indicator and baseline are drawn to show the asphaltene content of oil with respect to their refractive index. Furthermore, after mixing the samples of synthetic oils with acid solutions, droplets of remaining oil were taken to identify their refractive index. Results are classified in four different lines with y-intercept equals to the pure toluene refractive index (=1.496 @ T = 20 °C). These four lines are shown in Fig. 4a. The amount of asphaltene molecules which reacted to from acid induced sludge were determined by comparing the percentage of asphaltene content for equal refractive indexes from synthetic oil line and HCl acid percentage line. This comparison shows that approximately 0.7, 0.6 and 0.4 are the values of the remained asphaltene ration (amount of remained asphaltene in oil/amount of total asphaltene in oil) for HCl acid 10, 15 and 28 wt% respectively.

If the recorded refractive indexes are categorized by the percentage of solution asphaltene content, it will be obvious that the refractivity index increases with asphaltene content. The slope of the refractive index also decreases with an increase in the asphaltene content. Due to

Fig. 2. Conductivity vs. surfactant concentration.
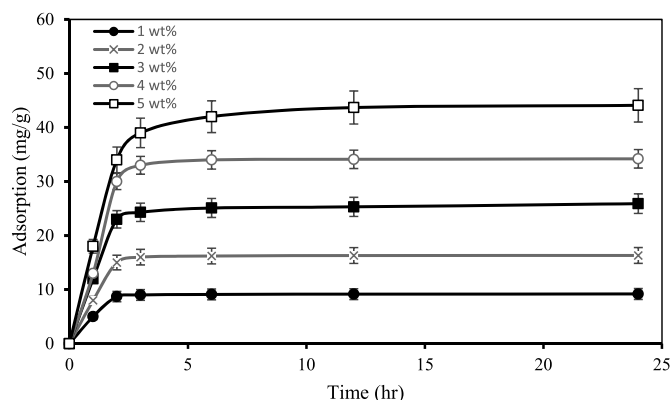
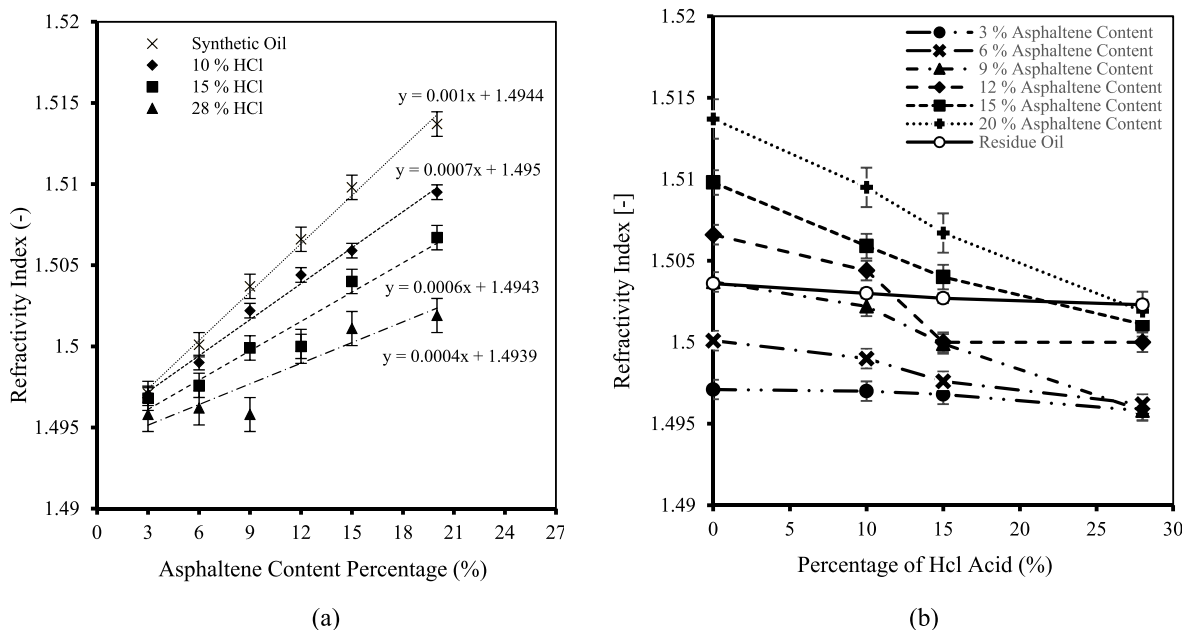**Fig. 3.** Adsorption of surfactant vs. time.

Fig. 4. (a) Effect of asphaltene content on refractivity index before and after treatment with different HCl acid concentration, (b) Effect of HCl acid concentration on refractivity index for different oil sample.
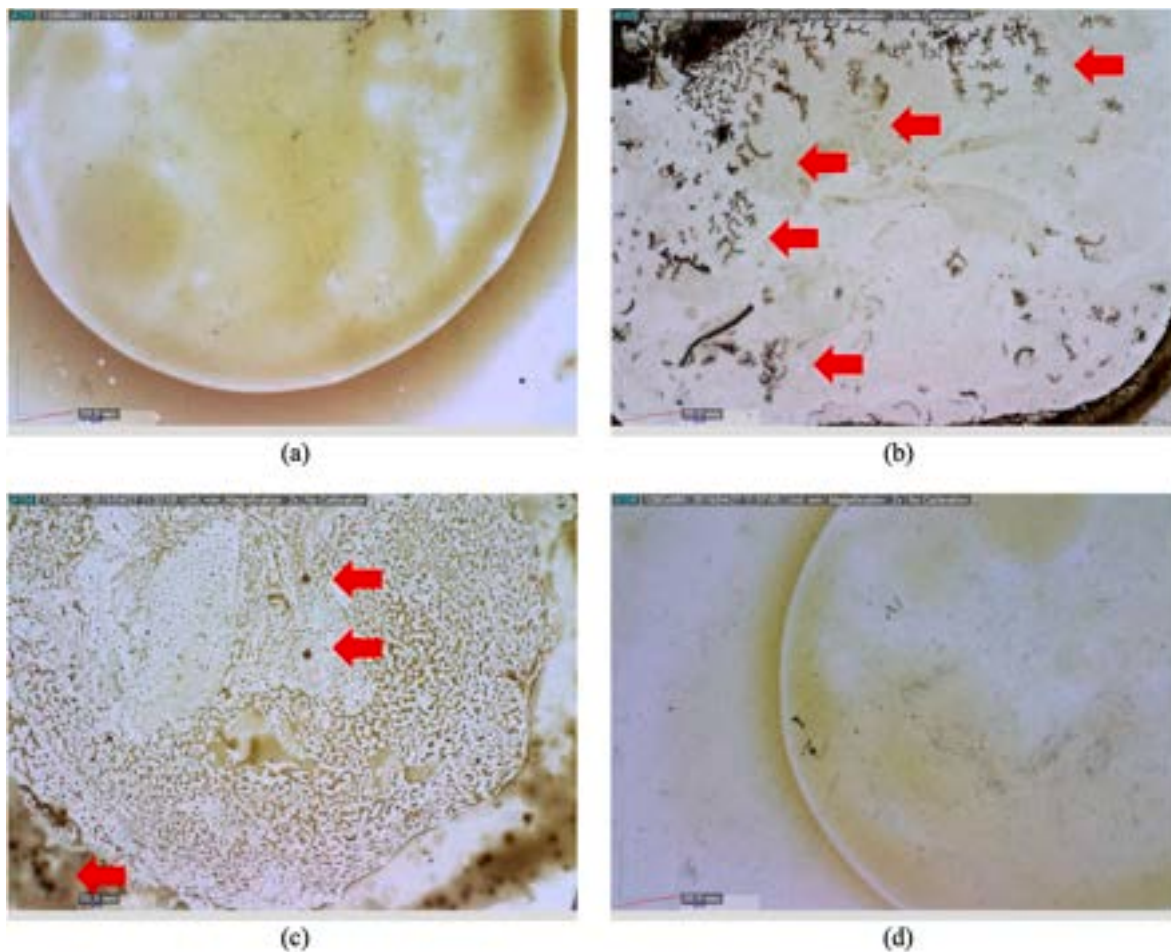

Fig. 5. Reaction of hydrochloric acid 15 wt% with (a) Aromatic, (b) Asphaltene, (c) Resin and (d) Saturated solutions.

the high concentration of asphaltene in medium, the probability of re-action between acid and asphaltene molecules increases. The refractive indexes of remaining oils with asphaltene concentration of 3, 6 and 9 wt % reacted with HCl 28 wt% are very close to that of pure toluene. Thus, it shows that almost all the asphaltene molecules are trapped as sludge in the emulsion phase. The carried out tests on the de-asphalted crude oil to examine the role of other components of crude oil reflected no sub-stantial changes in the respective refractive indexes. This fact reveals that asphaltene has the main role in the interaction of acid and oil because of its polarity and surface activity (Fig. 4b).

In addition, it was attempted to measure the effect of other oil components such as resins, saturates and aromatics. After preforming SARA test, each separated component was mixed with 15 wt% of hy-drochloric acid and further reaction was observed by microscope. As Fig. 5b depicts, acid presence stimulates the asphaltene molecules to become dramatically unstable in the liquid phase followed by resin being less affected by the acid (Fig. 5c). Compression with earlier, the other two components remained stable in acidic environmental condi-tions (Fig. 5a and d).

The pH values of acid solutions before and after mixing with pre-pared synthetic oil samples are measured and presented in Fig. 6. As the amount of asphaltene in the synthetic oil samples rises, the pH value rises as well. Increased asphaltene content enhances the possibility of an acid-asphaltene molecule reaction, resulting in a higher pH value. The similar pattern can be seen at all HCl concentrations. However, for so-lutions with higher concentration of HCl, they experience stronger increasing in pH value after treatment because of higher acidity.

Similarly, variations in pH value before and after applying bio-surfactant were recorded, but no significant differences were found. Because ZSCE molecules bind to asphaltene, the most polar and surface-active sub-fraction of the oil component, they prevent acid from reacting with it. With almost the same pH value, the acid solution stayed intact.

3.4. FT-IR spectrum

The effect of the acid on asphaltene metallic elements, nickel and vanadium was also studied using FT-IR method. The experiment was performed by adding acid to the asphaltene, stirring the resulting mixture and then filtration of it. Atomic absorption spectroscopy was used to determine the concentrations of V and Ni in acid (before and after addition to asphaltene), and the results are summarized in Table 3.

As can be seen in Table 3, in entry 2, after treatment of asphaltene with acid, the concentration of Ni decreased, and the concentration of V increased. This indicates that the treatment of the asphaltene with acid caused the V to be removed from asphaltene molecules, while some of the Ni in the acid was absorbed by these molecules. This difference can be attributed to the greater tendency of Ni in the formation of stable
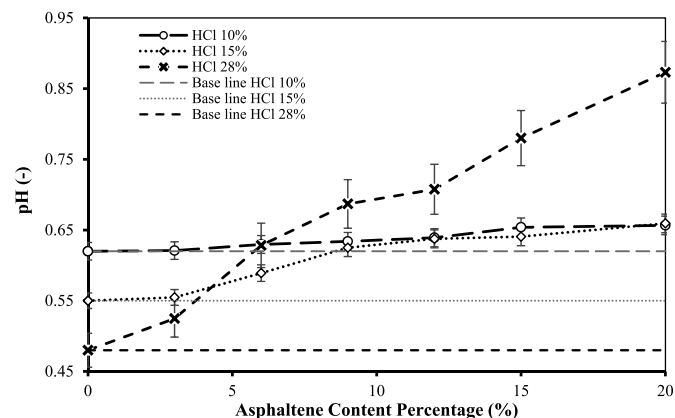
Table 3
Atomic absorption spectroscopy.

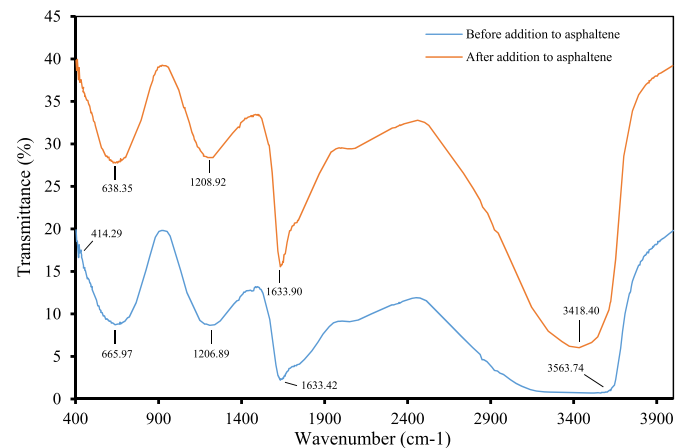| Entry	Acid	Ni Concentration (μg/L)	V Concentration (μg/L)
1	Acid before addition to asphaltene	36.70	0.83
2	Acid after addition to asphaltene	26.02	4.35

Fig. 7. The FT-IR spectrum of acid before and after addition to asphaltene.

complexes with asphaltene molecules. The electronic structure of Ni, and its higher electron affinity than V are probably the reason of this big difference in the complex formation. As it is clear from Fig. 7, there are no important differences in the FT-IR spectrums of acid before and after treatment with asphaltene thus it can be concluded that no organic molecule was dissolved in acid during treatment with asphaltene molecules.

3.5. Sludge volume measurement

Measured volume results indicate that sludge and emulsion volume is increased 113% by 28 wt% HCl acid while this value was 7% for 15 wt % HCl acid on average for all asphaltene concentrations. In fact, the formation of acid-induced sludge in high acid concentrations such as 28 wt% is significant. These values indicate the amount of sludge and formed emulsion at the interface between oil and water increases with asphaltene concentration. While results are recommended to use acid with low HCl concentration due to minor sludge formation, the strength of the acid solution must be sufficient to leave an appropriate influx through the matrix. Thus, the choice of 15 wt% HCl acid is a satisfactory option in routine jobs, however, the use of additives such as anti-sludge agents is crucial in operations.

Changing the concentration of asphaltene in synthetic oil from 15 wt % to 20 wt% does not significantly increase the volume of acid-induced sludge phase. This fact indicates that most of the acid influence is impressed with asphaltene concentration less than 15 wt%. Above this concentration, the acid solution does not act as the same and the volume of the sludge remains much lower. These results are displayed in Fig. 8a. Besides, the use of the both additives (i.e., commercial anti-sludge agent NE32 and bio-surfactant ZSCE) has prevented sludge formation so that no significant volume of sludge has been observed even in formed emulsion layer (Fig. 8b).

3.6. Contact angle measurement

Fig. 9a reveals that the contact angle increases by increasing aging time with sludge solution. The slope of the contact angle growth is
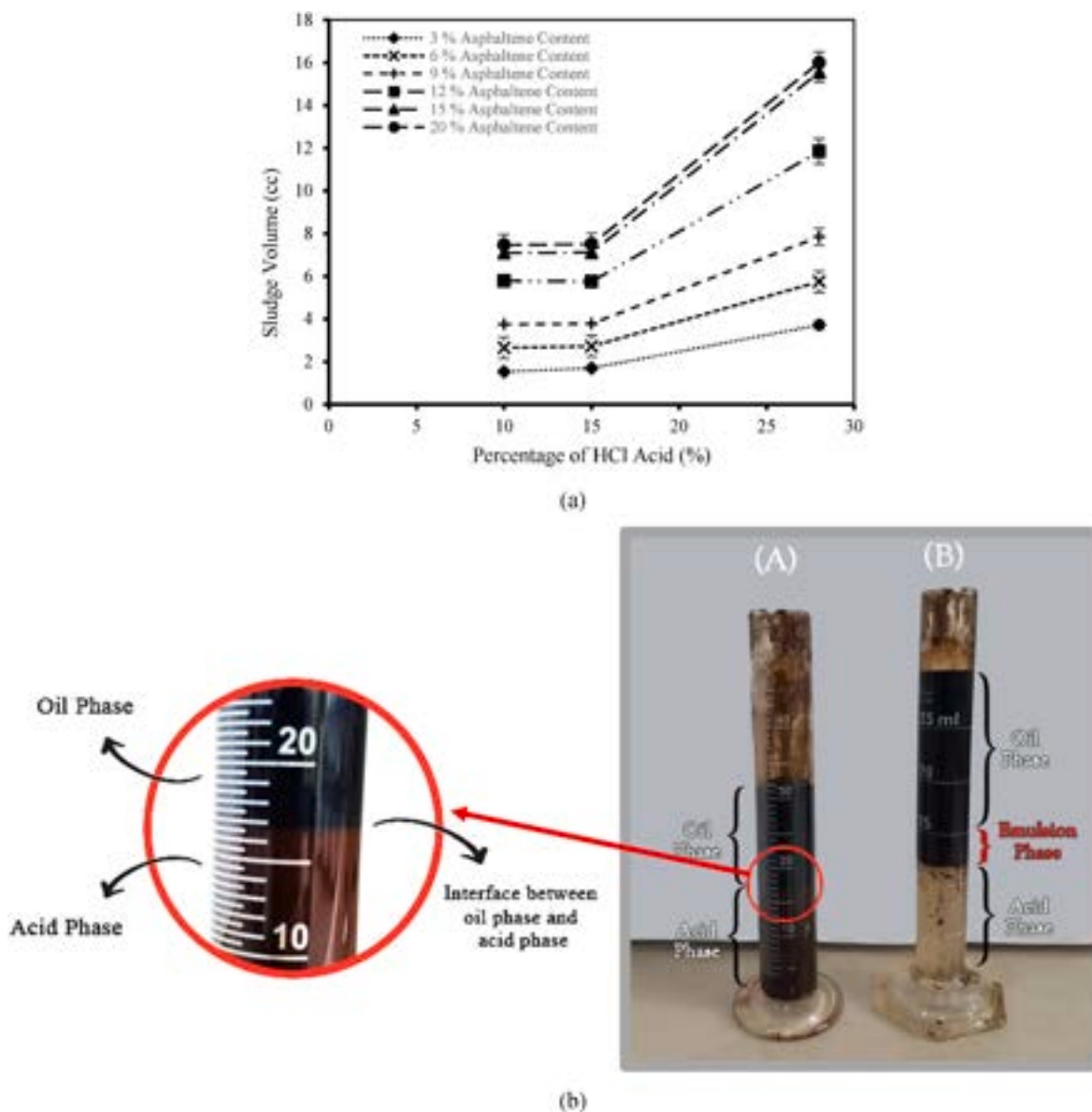

Fig. 6. pH value changes after treatment of different concentrations of HCl solutions with synthetic oil samples with different asphaltene contents.

Fig. 8. (a) Volume of formed emulsion phase and sludge for different types of synthetic oil and acid samples, (b) Usage of commercial bio surfactant (A) and anti-sludge agent (B).

higher in the first 30 min of aging time. The increase in the concentration of sludge in media from 1 wt% to 2 wt% leads to an increase in contact angle for each aged time and rock type. That indicates more sludge structures are adsorbed on the rock surface. Changing contact angle from water wet surface toward an oil wet one is noticeably displayed in Fig. 9c through 9e. The highest contact angle was observed for vuggy carbonate samples. The existence of large pore space in this rock type encourages the sludge phase to settle in and alter the wettability. This phenomenon is obvious in the higher concentration of sludge (Table 4.).

In Fig. 9b the effect of commercial surfactant WA120 and the bio-surfactant ZSCE on the contact angle of rock samples were shown and compared with the measurements without using surfactant and their initial condition. After 1 h of aging, both surfactants could stop the wettability alteration from being more oil-wet. In this case, the bio-surfactant ZSCE was more efficient, especially for vuggy carbonate rock. But after 2 h of aging, the commercial surfactant WA120 was unable to keep rock surface wettability oil-wet and failed. On the other hand, after the same course of treatment, no significant contact angle

changes were occurred by using bio-surfactant ZSCE.

As it was mentioned earlier, ZSCE molecules (i.e., saponins) consist of two parts: hydrophobic and hydrophilic parts. When acid solution containing dispersed ZSCE is mixed with crude oil, ZSCE molecules are adsorbed to most polar and surface-active sub-fraction of oil component, asphaltene, and do not allow acid to react with it. Even in the case of wettability alteration, ZSCE molecules are competing by their hydrophilic part with sludge structure for adsorption on the rock surface. Eventually, the hydrophilic part is adsorbed onto the rock surface part while the hydrophobic part is oriented towards the aqueous phase.

3.7. IFT measurement

One of the key mechanisms in post-flush in matrix acidizing is to reduce interfacial between aqueous phase and oleic phase tension by utilizing proper surfactant. As IFT is reduced, the capillary number is increased, leading to reduced residual organic phase saturation. Thus, the ability of surfactant to lower the IFT between the aqueous solution and oil phase is one of the most important aspects during post-flush stage
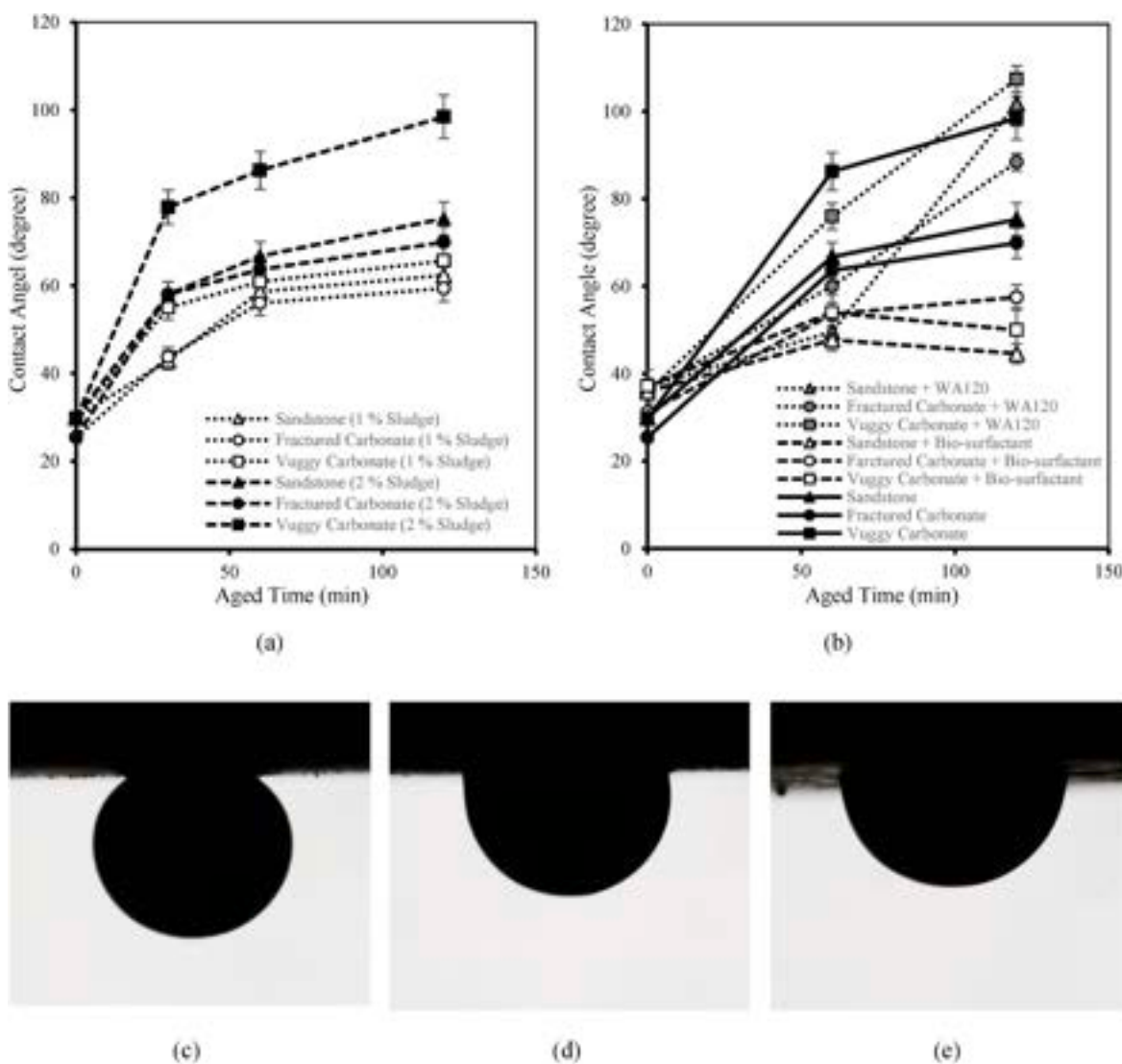
Fig. 9. (a) Effect of aging time on Wettability of different sludge concentration, (b) Effect of used commercial surfactant and bio-surfactant on wettability alteration, Contact angle measurement (c) Water-wet, (d) Neutral-wet and (e) Oil-wet.

of stimulation process. IFTs for common chemical surfactants in oil and gas industry and ZSCE bio surfactant in the presence of oil phase are shown in Fig. 10. Results display that there is not much difference in the interfacial tension reduction caused by bio-surfactant compared to other commercial surfactant. Therefore, due to the low price and availability of proposed bio-surfactant, its application is cost effective and hence recommended. In Fig. 10, the CMC$_{IFT}$ of ZSCE bio-surfactant is 490 ppm, approximately 3.2 wt%, which is similar to CMC determined by conductivity technique.

4. Molecular dynamic (MD) simulation

Designing and optimization processes of the materials which are considered in the simulation side of the present paper were performed using Material Studio 2017 (BOIVIA) software. Two different asphaltene structures available in Iranian oil reservoirs, Saponin, toluene, and calcite surface occupied the designed simulation cell spaces so that enables 6 defined scenarios to be evaluated in a meaningful approach. Fig. 11 illustrates the optimized structures of the above mentioned materials in terms of bonding energy and length, position of atoms in an individual structure, the bond angles (Takanohashi et al., 2004; Sheremata et al., 2004).

These two asphaltene structures have been selected in such a way that they are different in their functional groups (i.e. benzene, naphthalene, phenanthrene, phenylnapthalene, pyrene, diphenylnaphthalene, indole, dibenzothiophene, dibenzofuran and porphyrin). Also, each of them represents different size of asphaltene molecular structure. Asphltene type I has oxygen and nitrogen in its structure and asphaltene type II contains sulfur, nitrogen and vanadium as heavy metal elements.

The following simulations were relaxed by the canonical NVT ensemble (at a constant amount of substance (N), volume (V) and temperature (T)). The simulation temperature was adjusted to 298.15 K. Six different scenarios were designed to simulate the possibility of formation and prevention of sludge taking the role of asphaltene into account. Atomic based summation method using Particle Mesh Ewald for the reciprocal part was used to correct Long-range electrostatic interactions. All designed cases were run in a vacuum environment of 90 Å applying COMPASS force field (Sun et al., 1998). COMPASS force field is developed by combining ab initio and empirical parameterization techniques for atomistic simulations of common organic molecules, inorganic small molecules, and polymers (Sun et al., 1998; Sun, 1998). Particle motion is integrated using the leapfrog method with a time step of 1 fs. Accordingly, simulations lasted 500 ps to calculate the properties. Total energy in the used COMPASS force field accounts for the

Table 4
Thin-sections from three different rocks.

Aged Thin-sections in Sludge Solution with Different Times						
Reference Thin-sections	After 30 min aging		After 60 min aging		After 120 min aging	
	1 wt% sludge	2 wt% sludge	1 wt% sludge	2 wt% sludge	1 wt% sludge	2 wt% sludge
Sandstone						
Fractured Carbonate Rock						
Vuggy Carbonate Rock						

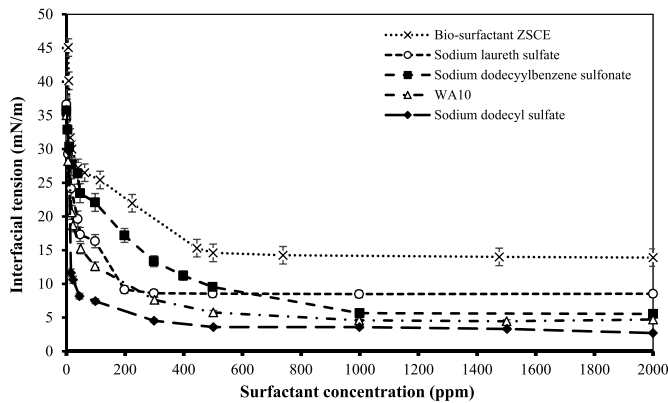| Aged Thin-sections by Surfactant and Sludge Solution						
Reference Thin-sections	WA 120 Surfactant			ZSCE Surfactant		
	After 0 min aging	After 60 min aging	After 120 min aging	After 0 min aging	After 60 min aging	After 120 min aging
Sandstone						
Fractured Carbonate Rock						
Vuggy Carbonate Rock						

Fig. 10. Comparison of IFT of ZSCE vs. industrial surfactants.

following energies:

$$E_{total} = E_{bond} + E_{angle} + E_{oop} + E_{torsion} + E_{cross} + E_{elec} + E_l \quad (2)$$

Where E_{bond}, E_{angle}, E_{oop}, $E_{torsion}$, E_{cross}, E_{elec} and E_l represent bond stretching energy, angle bending energy, out-of-plane angle coordinates, bond torsion energy and cross-term interacting energy, respectively (Liu et al., 2015). Initially, NPT ensemble was applied to mix the materials with 500,000 steps with pressure and temperature of 1 bar and 298 k, respectively, and then NVT ensemble was run to place the materials on the calcite slab. Cut-off distance of 12.5 Å and accuracy of 0.001 kcal/mol were used to be considered for long-range electrostatic interactions allowance for all boxes, van der Waals interaction and Ewald summation method, individually. Radial distribution function (RDF), g(r), shows the probability of the occurrence of a particle "a" at a specific

distance of "r" from particle "b" compared to the average number density. The following Eq. 4 is used to calculate g(r) of the system.

$$g(r) = \frac{1}{\rho 4\pi^2 \delta r} \frac{\sum_{t=1}^{T} \sum_{j=1}^{N} \Delta N(r \to r + \delta r)}{NT} \quad (3)$$

Where ρ, N, T, δr, ΔN, represent system density, number pf atoms, simulation total time initial interval distance and number of atoms between r and $r + \delta r$, respectively. Moreover, it is considered that the peak of each plot represents specific neighbor molecules which could well imitate the microscale configuration of aggregation or/and adsorption (Sheremata et al., 2004).

In the present study, two MD simulation scenarios were designed i) Two asphaltene structures (type I and II) were examined to determine the asphaltene type that has more possibility to precipitate after being mixed with HCl (cf. SM, S2, Table S2), ii) use the selected asphaltene molecules in presence of calcite rock surface and check the effect of Saponin molecules in induced sludge prevention (cf. SM, S2, Table S2).

4.1. Scenario 1

4.1.1. Asphaltene (type I) and hydrochloric acid

In the simulation cell including Asphaltene (I), HCl and toluene as the asphaltene solvent, after passing 500 ps the system reached the stable condition so that the thermodynamic parameters such as temperature, energy, and the density of the simulation boxes converged, balanced and stable condition achieved after 30 ps after stabilization stage (cf. SM, Fig. S6). The appeared RDF plot picks indicate two values of 2.8 Å and around 4.5 Å as the obtained picks for $N_{Asphaltene} - H_{HCl}$ and $O_{Asphaltene} - H_{HCl}$, respectively, implying the strong tendencies between Asphaltene (I) molecules and hydrogen bonds (Fig. 12a and b).
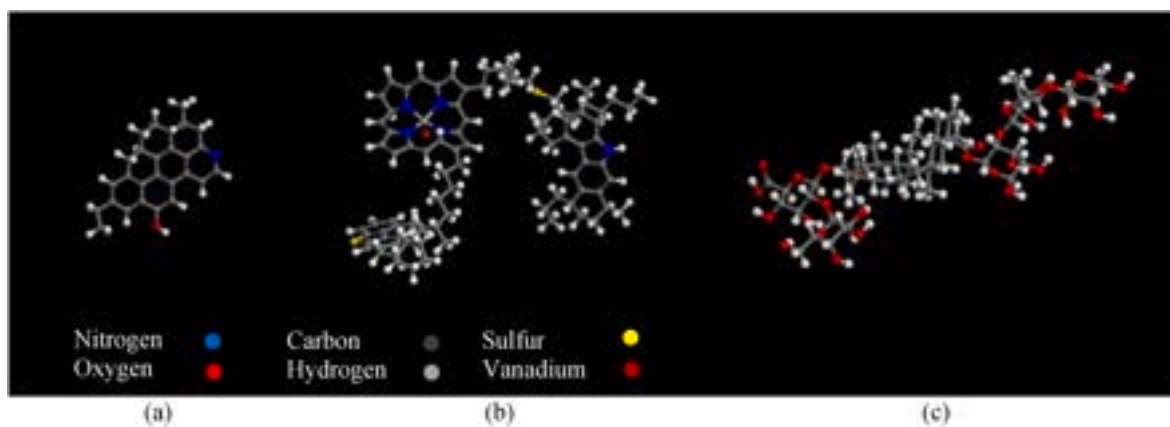
Fig. 11. Structure model of the used materials in MD simulations. (a) Asphaltene structure [type I], (b) Asphaltene structure [type II] (with heavy metal) and (c) Saponin structure (Ahmadi and Shadizadeh, 2013; Takanohashi et al., 2004; Sheremata et al., 2004).
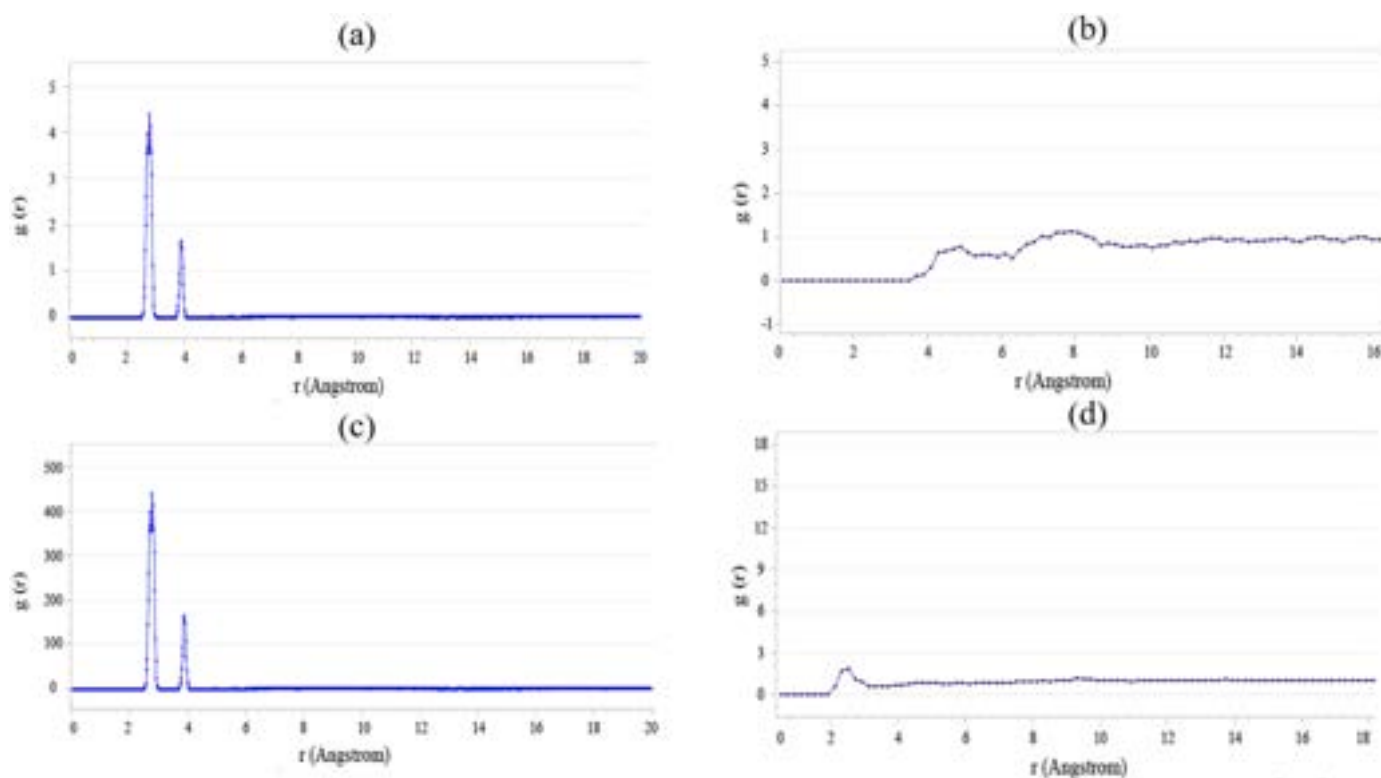

Fig. 12. Radial distribution of (a) $N_{Asphaltene(I)} - H_{HCl}$, (b) $O_{Asphaltene(I)} - H_{HCl}$, (c) $N_{Asphaltene(II)} - H_{HCl}$, (d) $O_{Asphaltene(II)} - H_{HCl}$.

4.1.2. Asphaltene (type II) and hydrochloric acid

In this step, Asphaltene (II) was exposed to HCl to check the affinity between the two structures. RDF results for $N_{Asphaltene} - H_{HCl}$ and $O_{Asphaltene} - H_{HCl}$ show the pick approximately equal values of 2 Å and 2.2 Å, respectively (Fig. 12c and d). In comparison with the results for Asphaltene (I) (Fig. 12a and b), these simulated RDFs revealed the higher tendencies of Nitrogen and Oxygen existed in Asphaltene (II) to form a hydrogen bond through the available hydrogen cations in the simulation cell and in turn, more probability of sludge formation. Hence, Asphaltene (II) was selected to conduct scenario 2.

4.2. Scenario 2

In this scenario, we tried to investigate the tendency of Asphaltene (II) and Saponin molecules to the calcite surface in conditions where i)

each one (either Asphaltene (II) or Saponin molecules) is present on the rock surface and ii) both of them are in exposure to the rock surface. Toluene molecules were also present as the solvent of Asphaltene (II) molecules (cf. SI, S2, Table S2). The distances of $C_{Asphaltene\ (II)} - Ca_{Calcite}$ and $C_{Saponin} - Ca_{Calcite}$ are approximately simulated equally ($r \approx 1.7$ Å). Nevertheless, as Fig. 13a and b depict, the g(r) value for $C_{Saponin} - Ca_{Calcite}$ is significantly over than that for $C_{Asphaltene\ (II)} - Ca_{Calcite}$. Despite the equal distance of the picks in both cases ($r \approx 1.7$ Å), this comparison highlights the more tendency of calcite structure to attract Saponin towards the surface which also represents a potential role of Saponin to decrease the wettability alteration of calcite slab by alleviating the Asphaltene deposition process.

Adding all the structures (i.e. Asphaltene (II), Saponin, and Toluene molecules on the calcite slab) to the simulation cell, yielded the shown RDF profiles for $C_{Asphaltene\ (II)} - Ca_{Calcite}$ and $C_{Asphaltene(II)} - C_{Saponin}$ in
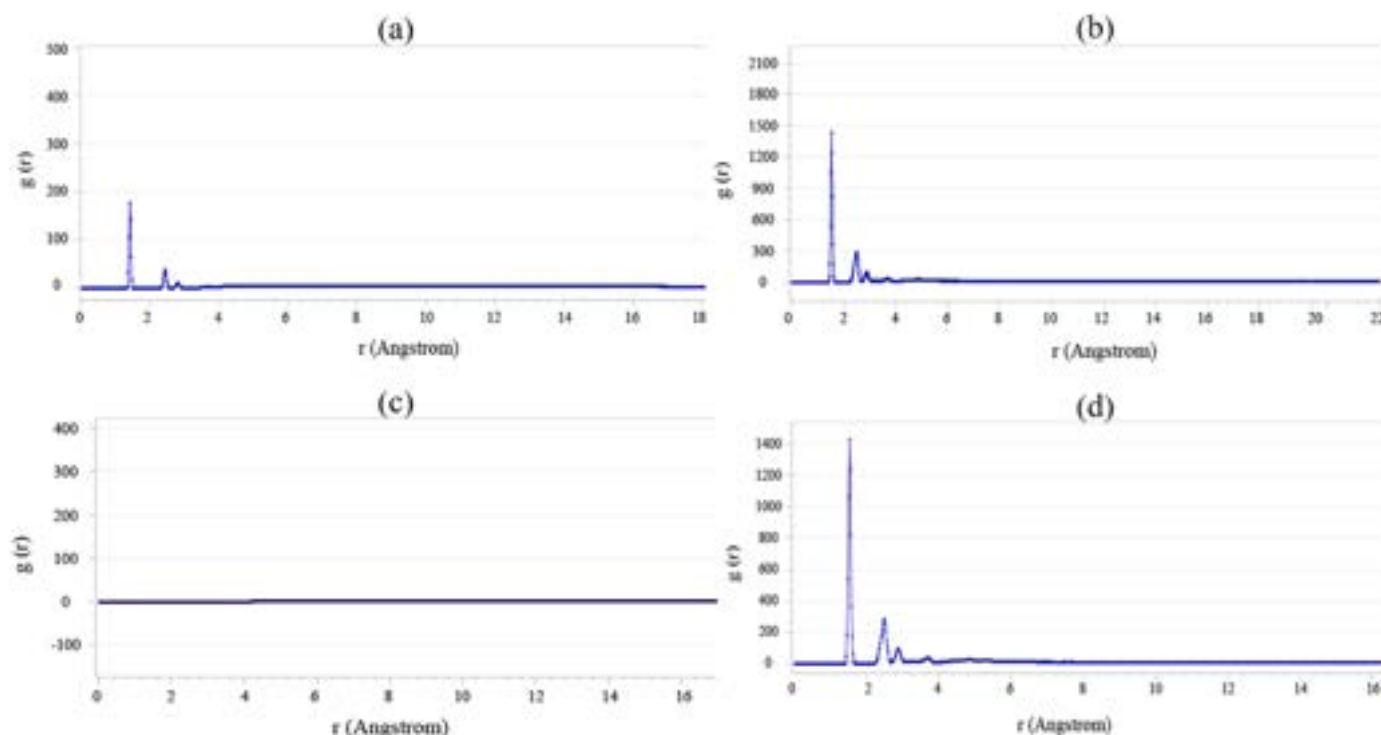
Fig. 13. RDFs of (a) $C_{Asphaltene(II)} - Ca_{Calcite}$, (b) $C_{Asphaltene(II)}$ and $C_{Saponin}$, (c) $C_{Asphaltene(II)} - Ca_{Calcite}$, (d) $C_{Asphaltene(II)} - C_{saponin}$.

Fig. 13c and d, respectively. While there is RDF pick at 1.7 Å in Fig. 13a, $C_{Asphaltene\ (II)} - Ca_{Calcite}$ formed a straight line with no pick (Fig. 13c) to highlight the role of Saponin presence in the simulation cell. On one hand, the tendency between $C_{Asphaltene(II)} - C_{Saponin}$ has weakened the interaction between $C_{Asphaltene\ (II)} - Ca_{Calcite}$, and on the other hand, the deviation of the asphaltene molecules affinity towards the Saponin molecules amplify the condition of less asphaltene deposition on the calcite surface and in turn, less wettability alteration towards water wetness. Comparison with the experimental findings, all these simulations results are in line with the results from the performed experiments in this study.

5. Conclusion

In the present study, the effects of sludge formation damage on the pay zone and its production were investigated. Since no substantial sludge is observed after mixing HCl acid with an asphaltene free crude oil, it is found to be a crucial component that forms induced sludge as a result of its interaction with injected acid during the field operations.

The amount of sludge increases significantly with an increase in the concentration of acid. Changing the wettability state towards oil-wetness after sludge deposition for all three types of used rocks in this paper represented the wettability state variation in oil reservoirs as another source of damage causing by sludge formation. In order to retain rock wettability to original water-wet state and to prevent formation of acid-induced sludge, two commercial surfactant and anti-sludge agent and the bio surfactant were examined. The commercial surfactant and bio-surfactant were able to maintain the rock water-wetness, however, in contrast to ZSCE bio-surfactant, the commercial one failed to maintain wettability state for a long aging time. Accordingly, the ZSCE bio-surfactant showed a better performance than the commercial ones to prevent the sludge formation. The results of molecular dynamic simulations show that hydrogen bond is the main force that actively leads to asphaltene deposition on the rock surface. Adding Saponin molecule to the simulation cells intervene in the interaction between calcite slap and Asphatene molecule as its affinity towards the calcite structure is higher

than that of asphaltene molecule and introduces the used bio-surfactant in this study as an effective sludge formation inhibitor in reservoirs.

Authorship contributions

Conception and design of study: Bahram Soltani Soulgani, Hamidreza Asaadian, Pouyan Ahmadi, Babak Mokhtari; Acquisition of data: Mohammad Zare Khormizi, Hamidreza Asaadian, Pouyan Ahmadi, Saba Mohammadi; Analysis and/or interpretation of data: Hamidreza Asaadian, Shirin Baghersaei, Pouyan Ahmadi. Drafting the manuscript: Hamidreza Asaadian, Pouyan Ahmadi, Bahram Soltani Soulgani, Babak Mokhtari; Revising the manuscript critically for important intellectual content: Bahram Soltani Soulgani, Hamidreza Asaadian, Pouyan Ahmadi, Babak Mokhtari. Approval of the version of the manuscript to be published (the names of all authors must be listed): Hamidreza Asaadian, Pouyan Ahmadi, Mohammad Zare Khormizi, Saba Mohammadi, Bahram Soltani Soulgani, Shirin Baghersaei, Babak Mokhtari.

Declaration of competing interest

The authors declare that they have no known competing financial interests or personal relationships that could have appeared to influence the work reported in this paper.

Data availability

No data was used for the research described in the article.

contributions from non-authors.

Nomenclature

C	Carbon
C	Light speed, [L/t], (ft/sec)
Ca	Calcium
E	Energy, [M*L/t], (kcal/mol)
H	Hydrogen
O	Oxygen
N	Nitrogen
N	Refractivity index, [dimensionless]
N	Number of atoms
T	Simulation total time [t]
ρ	System density, [M/L^3]
υ	Light speed in medium, [L/t], (ft/sec)
δr	Interval distance [L]
ΔN	Number of atoms between r and $r + \delta r$

Appendix A. Supplementary data

Supplementary data to this article can be found online at https://doi.org/10.1016/j.petrol.2022.111009.

References

Abdollahi, R., Shadizadeh, S., 2012. Effect of acid additives on anticorrosive property of henna in regular mud acid. Sci. Iran. 19 (6), 1665–1671.

Adams, J.J., 2014. Asphaltene adsorption, a literature review. Energy Fuel. 28 (5), 2831–2856.

Aghajanzadeh, M.R., et al., 2019. Wettability modification of oil-wet carbonate reservoirs using silica-based nanofluid: an experimental approach. J. Petrol. Sci. Eng. 178, 700–710.

Ahmadi, M.A., Shadizadeh, S.R., 2013. Experimental investigation of adsorption of a new nonionic surfactant on carbonate minerals. Fuel 104, 462–467.

Ahmadi, M.A., Galedarzadeh, M., Shadizadeh, S.R., 2015. Wettability alteration in carbonate rocks by implementing new derived natural surfactant: enhanced oil recovery applications. Transport Porous Media 106 (3), 645–667.

Ahmadi, P., et al., 2019a. Investigation of the simultaneous chemicals influences to promote oil-in-water emulsions stability during enhanced oil recovery applications. J. Mol. Liq. 275, 57–70.

Ahmadi, P., et al., 2019b. A new approach for determination of carbonate rock electrostatic double layer variation towards wettability alteration. J. Mol. Liq. 275, 682–698.

AlMubarak, T., et al., 2015. Investigation of acid-induced emulsion and asphaltene precipitation in low permeability carbonate reservoirs. In: SPE Saudi Arabia Section Annual Technical Symposium and Exhibition. OnePetro.

Almubarak, T., et al., 2021. Matrix acidizing: a laboratory and field investigation of sludge formation and removal of oil-based drilling mud filter cake. SPE Drill. Complet. 36 (2), 281–299.

Asaadian, H., Soulgani, B., 2016. Carbonate acidizing optimazation in Iranian oil field. In: 78th EAGE Conference and Exhibition 2016. European Association of Geoscientists & Engineers.

Asaadian, H., Soulgani, B., Sahnalizadeh, A., 2017a. Experimental study on acidizing fluid viscosity variation during carbonate well stimulation. In: 79th EAGE Conference and Exhibition 2017. European Association of Geoscientists & Engineers.

Asaadian, H., Soltani Soulgani, B., Karimi, A., 2017b. An experimental study on electrical effect on asphaltene deposition. Petrol. Sci. Technol. 35 (24), 2255–2261.

Ayirala, S.C., Vijapurapu, C.S., Rao, D.N., 2006. Beneficial effects of wettability altering surfactants in oil-wet fractured reservoirs. J. Petrol. Sci. Eng. 52 (1–4), 261–274.

Azari, V., et al., 2018. Electrokinetic properties of asphaltene colloidal particles: determining the electric charge using micro electrophoresis technique. Colloids Surf. A Physicochem. Eng. Asp. 541, 68–77.

Bognolo, G., 1999. Biosurfactants as emulsifying agents for hydrocarbons. Colloids Surf. A Physicochem. Eng. Asp. 152 (1–2), 41–52.

Campbell, G., 2002. Sludge Liquefaction Process and Agent, vol. 6. Patent US.

Chang, C.-L., Fogler, H.S., 1994. Stabilization of asphaltenes in aliphatic solvents using alkylbenzene-derived amphiphiles. 1. Effect of the chemical structure of amphiphiles on asphaltene stabilization. Langmuir 10 (6), 1749–1757.

Deymeh, H., Shadizadeh, S., Motafakkerfard, R., 2012. Experimental investigation of Seidlitzia rosmarinus effect on oil–water interfacial tension: useable for chemical enhanced oil recovery. Sci. Iran. 19 (6), 1661–1664.

Dyer, R.J., 1997. Anionic Compositions for Sludge Prevention and Control during Acid Stimulation of Hydrocarbon Wells. Google Patents.

Frenier, W.W., Hill, D.G., 2002. Effect of acidizing additives on formation permeability during matrix treatments. In: International Symposium and Exhibition on Formation Damage Control. OnePetro.

Garrouch, A.A., Jennings Jr., A.R., 2017. A contemporary approach to carbonate matrix acidizing. J. Petrol. Sci. Eng. 158, 129–143.

Garrouch, A.A., Malallah, A., Al-Enizy, M., 2006. An empirical model for predicting crude sludging potential caused by acidizing. In: SPE Annual Technical Conference and Exhibition. OnePetro.

Hashmi, S.M., Firoozabadi, A., 2013. Self-assembly of resins and asphaltenes facilitates asphaltene dissolution by an organic acid. J. Colloid Interface Sci. 394, 115–123.

Houchin, L., et al., 1990. The occurrence and control of acid-induced asphaltene sludge. In: SPE Formation Damage Control Symposium. OnePetro.

Jacobs, I., Thorne, M., 1986. Asphaltene precipitation during acid stimulation treatments. In: SPE Formation Damage Control Symposium. OnePetro.

Karimi, M., Shirazi, M.M., Ayatollahi, S., 2018. Investigating the effects of rock and fluid properties in Iranian carbonate matrix acidizing during pre-flush stage. J. Petrol. Sci. Eng. 166, 121–130.

Khurshid, I., et al., 2022. A numerical approach to investigate the impact of acid-asphaltene sludge formation on wormholing during carbonate acidizing. J. Energy Resour. Technol. 144 (6).

Knopp, M.S., 2009. Non-emulsifying Anti-sludge Composition for Use in the Acid Treatment of Hydrocarbon Wells. Google Patents.

Kudrashou, V.Y., Nasr-El-Din, H.A., 2019. Formation damage and compatibility issues associated with use of corrosion inhibitors in well acidizing-A review. In: SPE/ICoTA Well Intervention Conference and Exhibition. OnePetro.

Langevin, D., Argillier, J.-F., 2016. Interfacial behavior of asphaltenes. Adv. Colloid Interface Sci. 233, 83–93.

Liu, J., Zhao, Y., Ren, S., 2015. Molecular dynamics simulation of self-aggregation of asphaltenes at an oil/water interface: formation and destruction of the asphaltene protective film. Energy Fuel. 29 (2), 1233–1242.

Looney, J.R., McDougall, L.A., 1984. Use of Esters of Sulfonic Acids as Anti-sludge Agents during the Acidizing of Formations Containing Sludging Crude Oils. Google Patents.

Lu, Z., et al., 2021. Oil recovery from polymer-containing oil sludge in oilfield by thermochemical cleaning treatment. Colloids Surf. A Physicochem. Eng. Asp. 611, 125887.

Maley, D., et al., 2015. Acid additives effect on production–A beaverhill lake case study. In: SPE/CSUR Unconventional Resources Conference. OnePetro.

McLeod, H.O., 1984. Matrix acidizing. J. Petrol. Technol. 36 (12), 2055–2069.

Mirvakili, A., Rahimpour, M.R., Jahanmiri, A., 2012. Effect of a cationic surfactant as a chemical destabilization of crude oil based emulsions and asphaltene stabilized. J. Chem. Eng. Data 57 (6), 1689–1699.

Moore, E., Crowe, C., Hendrickson, A., 1965. Formation, effect and prevention of asphaltene sludges during stimulation treatments. J. Petrol. Technol. 17 (9), 1023–1028.

Morales, R., Diaz, C., 2017. Microemulsion additive to mitigate impacts of acid flow back. In: Abu Dhabi International Petroleum Exhibition & Conference. OnePetro.

O'Neil, B., Maley, D., Lalchan, C., 2015. Prevention of acid-induced asphaltene precipitation: a comparison of anionic vs. cationic surfactants. J. Can. Petrol. Technol. 54 (1), 49–62.

Olayiwola, S.O., Dejam, M., 2019. A comprehensive review on interaction of nanoparticles with low salinity water and surfactant for enhanced oil recovery in sandstone and carbonate reservoirs. Fuel 241, 1045–1057.

Pordel Shahri, M., Shadizadeh, S., Jamialahmadi, M., 2012. A new type of surfactant for enhanced oil recovery. Petrol. Sci. Technol. 30 (6), 585–593.

Rabie, A.I., Nasr-El-Din, H.A., 2015. Effect of acid additives on the reaction of stimulating fluids during acidizing treatments. In: SPE North Africa Technical Conference and Exhibition. OnePetro.

Shafiq, M.U., Mahmud, H.B., 2017. Sandstone matrix acidizing knowledge and future development. J. Pet. Explor. Prod. Technol. 7 (4), 1205–1216.

Shahsavani, B., et al., 2019. A conceptual modeling to predict asphaltene molecules fate within an annulus control volume. J. Mol. Liq. 292, 111414.

Sheremata, J.M., et al., 2004. Quantitative molecular representation and sequential optimization of Athabasca asphaltenes. Energy Fuel. 18 (5), 1377–1384.

Shirazi, M.M., Ayatollahi, S., Ghotbi, C., 2019. Damage evaluation of acid-oil emulsion and asphaltic sludge formation caused by acidizing of asphaltenic oil reservoir. J. Petrol. Sci. Eng. 174, 880–890.

Singh, S., 2002. Refractive index measurement and its applications. Phys. Scripta 65 (2), 167.

Stanimirova, R., et al., 2011. Surface rheology of saponin adsorption layers. Langmuir 27 (20), 12486–12498.

Sun, H., 1998. COMPASS: an ab initio force-field optimized for condensed-phase applications overview with details on alkane and benzene compounds. J. Phys. Chem. B 102 (38), 7338–7364.

Sun, H., Ren, P., Fried, J., 1998. The COMPASS force field: parameterization and validation for phosphazenes. Comput. Theor. Polym. Sci. 8 (1–2), 229–246.

Takanohashi, T., Sato, S., Tanaka, R., 2004. Structural relaxation behaviors of three different asphaltenes using MD calculations. Petrol. Sci. Technol. 22 (7–8), 901–914.

Taylor, K., Al-Ghamdi, A., Nasr-El-Din, H., 2003. Effect of rock type and acidizing additives on acid reaction rates using the rotating disk instrument. In: International Symposium on Oilfield Chemistry. OnePetro.

Weidner, J., 2011. Chemical Additive Selection in Matrix Acidizing.

Wong, T., et al., 1996. Acid sludge characterization and remediation improve well productivity. In: Permian Basin Oil and Gas Recovery Conference. OnePetro.

Wong, T., et al., 1997. Acid-Sludge characterization and remediation improve well productivity and save costs in the permian basin. SPE Prod. Facil. 12 (1), 51–58.

Xie, T., et al., 2005. A laboratory and modeling investigation of acid-created wormholes in sandstones. In: SPE European Formation Damage Conference. OnePetro.